Am. J. Hum. Genet. 67:822–831, 2000

Distinct Mutations in the Receptor Tyrosine Kinase Gene *ROR2* Cause Brachydactyly Type B

Georg C. Schwabe,[1] Sigrid Tinschert,[2] Christian Buschow,[8] Peter Meinecke,[3] Gerhard Wolff,[4] Gabriele Gillessen-Kaesbach,[5] Michael Oldridge,[6] Andrew O. M. Wilkie,[6] Reyhan Kömec,[7] and Stefan Mundlos[1,2,8]

[1]Max Planck Institut für Molekulare Genetik and [2]Institut für Medizinische Genetik, Charité, Berlin; [3]Altonaer Kinderkrankenhaus, Hamburg; [4]Institut für Humangenetik Universität Freiburg, Freiburg, Germany; [5]Institut für Humangenetik, Universitätsklinikum Essen, Essen, Germany; [6]Institute of Molecular Medicine, John Radcliffe Hospital, Oxford; [7]Kinderklinik Universitätsklinikum Mannheim, Mannheim, Germany; and [8]Universitätskinderklinik Mainz, Mainz, Germany

Brachydactyly type B (BDB) is an autosomal dominant skeletal disorder characterized by hypoplasia/aplasia of distal phalanges and nails. Recently, heterozygous mutations of the orphan receptor tyrosine kinase (TK) *ROR2*, located within a distinct segment directly after the TK domain, have been shown to be responsible for BDB. We report four novel mutations in *ROR2* (two frameshifts, one splice mutation, and one nonsense mutation) in five families with BDB. The mutations predict truncation of the protein within two distinct regions immediately before and after the TK domain, resulting in a complete or partial loss of the intracellular portion of the protein. Patients affected with the distal mutations have a more severe phenotype than do those with the proximal mutation. Our analysis includes the first description of homozygous BDB in an individual with a 5-bp deletion proximal to the TK domain. His phenotype resembles an extreme form of brachydactyly, with extensive hypoplasia of the phalanges and metacarpals/metatarsals and absence of nails. In addition, he has vertebral anomalies, brachymelia of the arms, and a ventricular septal defect—features that are reminiscent of Robinow syndrome, which has also been shown to be caused by mutations in *ROR2*. The BDB phenotype, as well as the location and the nature of the BDB mutations, suggests a specific mutational effect that cannot be explained by simple haploinsufficiency and that is distinct from that in Robinow syndrome.

Introduction

Brachydactyly is shortening of the digits that is due to abnormal development of the phalanges and/or metacarpals. It may occur as an isolated trait or as part of complex malformation syndromes. According to their patterns of skeletal involvement, heritable brachydactylies have been classified into the subtypes A–E (Bell 1951). Autosomal dominant brachydactyly type B (BDB [MIM 113000]) is readily distinguished from other brachydactylies by the characteristic shortening/hypoplasia of the distal phalanges, the occurrences of nail dysplasia, hypoplasia of middle phalanges, and variable degrees of distal and proximal symphalangism. Broad thumbs with or without distal duplication/clefts and syndactyly can be additional findings.

A locus for BDB was previously assigned to chromosome 9q22 (Gong et al. 1999; Oldridge et al. 1999). Mutation analysis of the *ROR2* gene, localized to 9q22 by radiation-hybrid mapping, in three unrelated families with BDB, revealed heterozygous missense and frameshift mutations within a distinct segment of the 943-amino-acid protein (Oldridge et al. 2000). ROR2 belongs to a family of receptor tyrosine kinases (RTKs), characterized by a cytoplasmic tyrosine kinase (TK) domain, distally located serine-threonine–rich and proline-rich domains, and distinct extracellular domains (Masiakowski and Carroll 1992). The function of ROR2 has been elucidated by the generation of mice with inactivated *Ror2* alleles, which results in a severe skeletal phenotype with foreshortened and misshapen bones and abnormal growth-plate morphology, indicating that *Ror2* is essential for normal chondrocyte differentiation (DeChiara et al. 2000; Takeuchi et al. 2000). However, in contrast with dominant BDB, mice heterozygous for the *Ror2* mutation ($Ror2^{+/-}$) have no phenotype, and homozygous mice ($Ror2^{-/-}$) have normal distal phalanges and thus lack the typical BDB features. Furthermore, mutations in *ROR2* have been identified in recessive Robinow syndrome (Afzal et al. 2000; van Bokhoven et al. 2000), but neither patients with Robinow syndrome nor the heterozygous carriers have BDB. The absence of any hand phenotype in individuals with chro-

Received June 23, 2000; accepted for publication August 17, 2000; electronically published September 12, 2000.

Address for correspondence and reprints: Stefan Mundlos, Max Planck Institut für Molekulare Genetik, Ihnestrasse 73, 14195 Berlin, Germany. E-mail: mundlos@molgen.mpg.de

0002-9297/2000/6704-0007$02.00

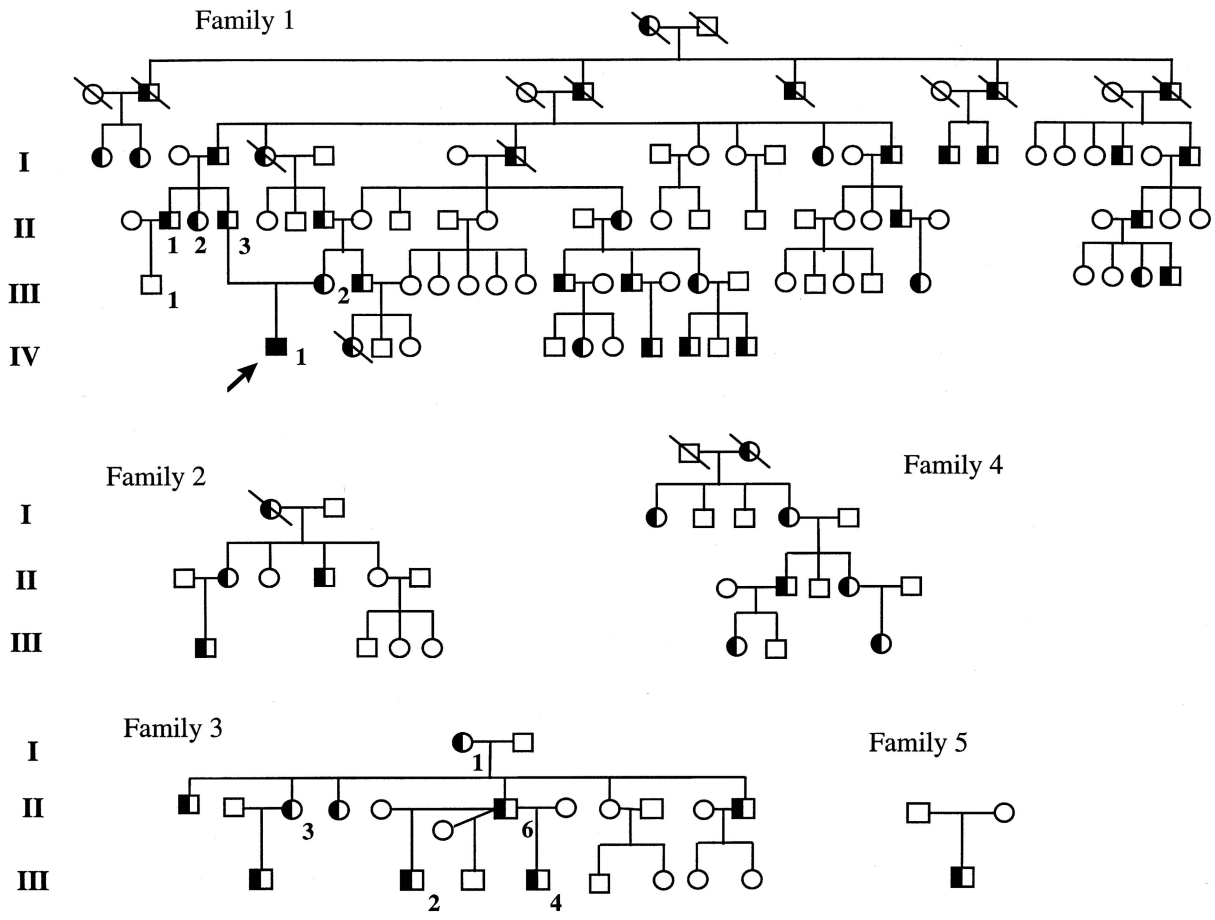

Figure 1 Pedigrees of families 1–5 with BDB. The homozygous individual is indicated by an arrow.

mosomal deletions involving *ROR2* (Oldrigde et al. 1999) is further support for the assumption that BDB is caused by a specific mutational effect that is different from simple haploinsufficiency.

In this report, we present four novel heterozygous mutations in *ROR2* that are predicted to result in a partial or complete truncation of the intracellular portion of the ROR2 protein, extending the known mutational spectrum in BDB. One individual with a homozygous *ROR2* mutation was identified. This patient shows a severe phenotype, which consists of an extreme form of brachydactyly with profound hypoplasia of hands and feet. In addition, he has features that show some degree of overlap with Robinow syndrome, such as vertebral anomalies, brachymelia of the arms, and a ventricular septal defect.

Patients and Methods

Clinical Description

Pedigrees of the five families investigated are shown in figure 1.

Family 1 is a large pedigree that originated in Turkey. Affected individuals exhibit typical features of BDB, which include bilateral hypoplasia of distal and middle phalanges of fingers and of toes 2–5, to a varying degree, and hypoplasia of nails on the corresponding rays. Radiographs were obtained from the parents (III/2 and II/3) of individual IV/1; all others were inspected visually. No other cosegregating medical problems were reported. One affected individual from a consanguineous union of an affected and an unaffected family member suffered from a Potter sequence and died on the 1st day of life.

One male individual (IV/1), the offspring of a consanguineous union of two affected individuals (II/3 and III/2), showed severe skeletal defects, primarily affecting the distal limbs and the spine (fig. 2). At birth, profound hypoplasia of hands and feet was noted; the nails were completely absent, with the exception of rudiments on the great toes. Skin defects were observed at the distal middle toes; these defects disappeared within a few weeks. Serial X-rays performed at age $\leqslant$7 years showed complete absence or severe hypoplasia of the distal and middle phalanges and, in some fingers and toes, absence

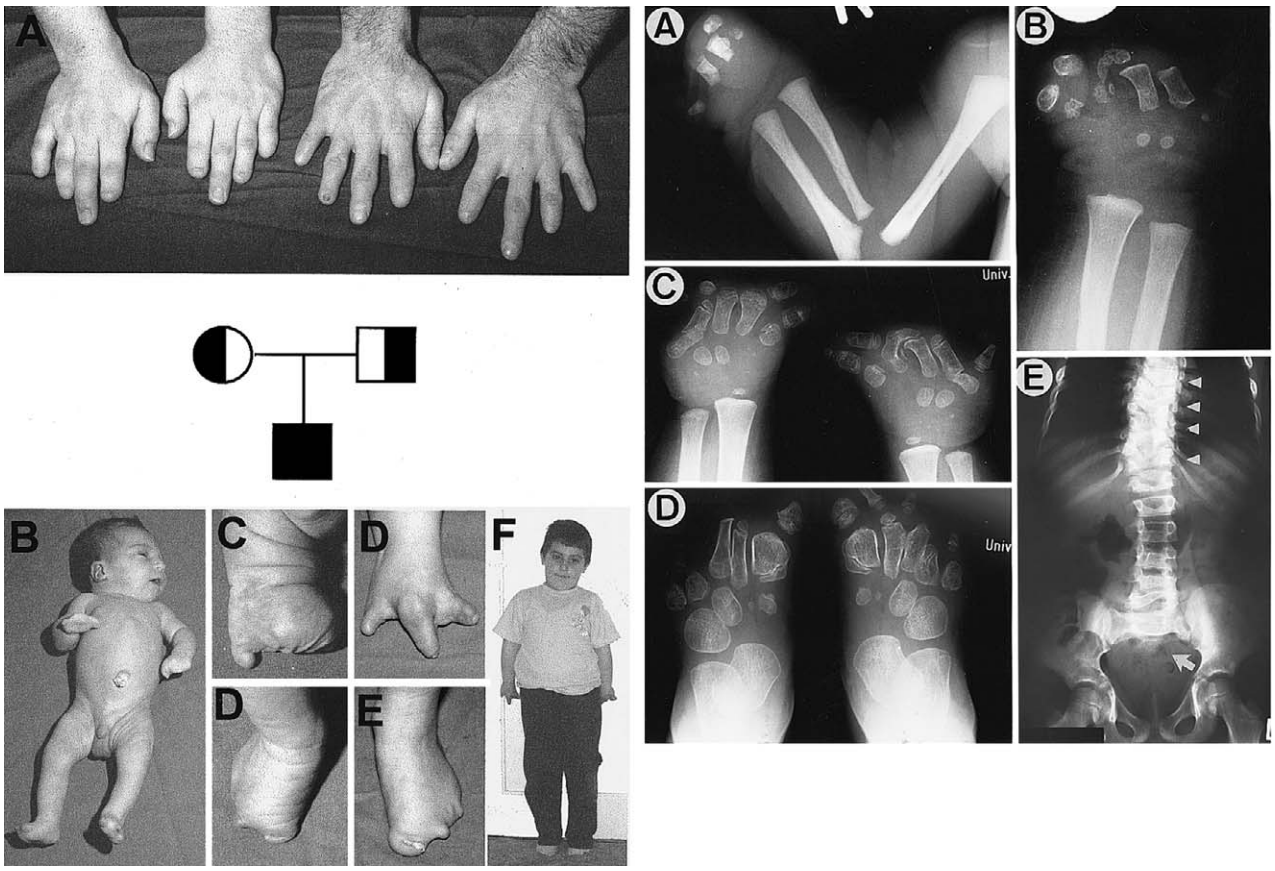

Figure 2 *Left,* Parents with BDB and their affected child, from family 1. Molecular analysis in this family revealed a 5-bp deletion in exon 8 of *ROR2,* with individual IV/1 being homozygously affected. Note the characteristic phenotype in the parents (*A*), with distal hypoplasia of phalanges 2, 4, and 5, nail dysplasia, and distal symphalangism. Their son shows a severe reduction deformity of all limbs. *B,* Presentation at birth. Corresponding pictures of the right hand (*C*) and foot (*D*) demonstrate almost complete absence of phalanges and nails. Also shown are the right hand after several orthopedic hand operations (*E*) and of the foot (*F*), as well as total-body view (*G*) of same patient at age 7.5 years. Note brachymelia of arms. *Right,* Radiological features of homozygously affected individual. *A,* Humerus, radius, ulna, and hand, after birth. Note normal structure but shortness of long bones and absence/hypoplasia of phalanges and metacarpals. *B,* Right hand at age 6 mo. *C,* Hands at age 2.5 years. *D,* Feet at age 2.5 years. Note complete disorganization and partial fusion of metacarpals, as well as shortening and cubic deformation of metatarsals. *E,* Anterior-posterior radiograph of thoracic and lumbar spine at age 7.5 years. Note the presence of multiple vertebral malformations, between T6 and T12 (*arrowheads*) and at L5/6, and hypoplasia of the sacrum (*arrow*).

of the proximal phalanges (fig. 2). The metacarpals and metatarsals were of normal number but were hypoplastic and deformed, and some had the characteristics of carpal bones. The long bones of the upper limbs were normal in structure and shape but short. Bone age, as judged by the appearance of ossification centers in carpal bones and the radial epiphysis, was normal. The birth weight and length, as well as growth, were within the normal range (15th percentile for Turkish boys; 3d percentile for boys from northern European background). The head circumference was normal at birth (25th percentile) and grew along the 50th percentile thereafter. The anterior fontanelle was large at birth (5 cm × 5 cm; >97th percentile) and was not completely closed at age 7.5 years. The measurement of individual skeletal elements revealed considerable disproportion. At age 7.5 years, lower arm length was 15.5 cm (2.25 cm; <5th percentile) and upper arms measured 21.5 cm (2 cm; <5th percentile), but the length of the legs was normal. The parents' total-body and upper-limb length were within normal limits. Radiographs of the spine showed vertebral segmentation defects of the lower thoracic spine (T8–T12), with hemivertebrae and fusions, as well as a malformation of L6/S1, with a resulting thoracolumbar scoliosis. The sacrum was hypoplastic. There were no neurological deficiencies, and the function of bladder and rectum was normal. A small penis was noted, and the testes were descended. Renal ultrasound performed after birth was normal. At age 7.5 years, the patient had borderline hypertelorism (95th percentile for interpupillary distance and intercanthal distance), a short narrow nose with a short columella, hyperplastic alveolar ridges, and severe caries of the deciduous teeth. None of the permanent teeth had erupted by age 7.5

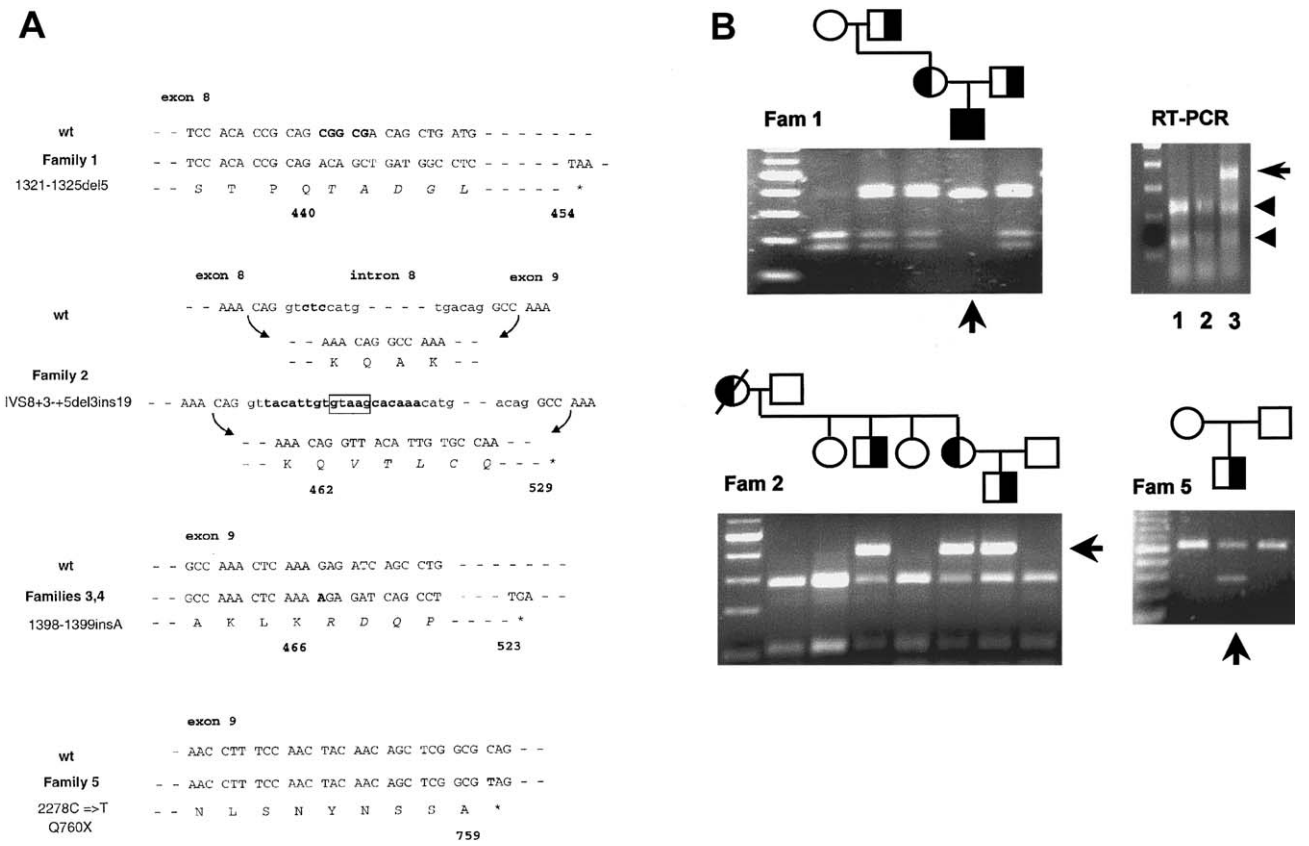

Figure 3 *ROR2* mutations in families with BDB. *A,* wt sequences are shown in the top line of each set; the mutated sequence is in boldface, exon sequences are in capital letters, and intron sequences are in lowercase. The predicted amino acid sequence of the mutated allele is shown in the bottom line of each set, with the altered sequence in italics. The mutation in family 1 is a 5-bp deletion (1321–1325del5) in exon 8, resulting in a frameshift and in a stop codon after 14 amino acids. Family 2 has an alteration in intron 8, which deletes 3 bp (CTC) and inserts 19 bp (IVS8+3 → +5del3ins19) at the 5′ splice site. This changes the wt splice site and results in the generation of an aberrant splice product using a new splice-donor site with a perfect consensus sequence (*boxed*). Families 3 and 4 have a 1-bp insertion (1398–1399insA) at the 5′ end of exon 9, resulting in a frameshift and in a premature termination codon after 57 amino acids. A 2278C→T missense mutation was detected in family 5, resulting in a stop codon at position Q760X. *B,* Gel analysis of PCR-amplified mutant region in families 1, 2, and 4. The 5-bp frameshift mutation in family 1 deletes a site for *Mwo*I, which cuts the wt sequence into two fragments. The unaffected family member (*left lane*) shows complete digestion, the heterozygous members show partial digestion, and the homozygous patient (*arrow*) shows no digestion. The RT-PCR product from a heterozygous family member containing the mutated region resulting in a 334-bp fragment was digested with *Mwo*I (*lane 3*) and was compared with controls (*lanes 1* and *2*). The undigested fragment (*arrow*), which corresponds to the mutated allele, is of an intensity approximately equal to that of the two digested wt fragments together (223 and 111 bp, *arrowheads*). The controls show complete digestion. The splice-site mutation in family 2 removes a *Bsa*I restriction site. The wt allele is cut into two fragments, of 271 and 113 bp, whereas the mutant allele remains undigested (*arrow*). The affected son in family 5 has a C→T transition at codon 2278. This nucleotide change creates a new restriction site for *Acc*I, which cuts the PCR-amplified sequence into two fragments of similar size (*arrow*). Amplified DNA from unaffected parents is not cut. Molecular-size markers are shown on the left.

years. The palate and uvula appeared normal. A small ventricular septal defect and a first-degree atrioventricular block were detected. Developmental milestones were normal. The patient's intellectual and motor development was normal, and he speaks fluent Turkish and German. After several orthopedic operations he has become able to use his hand to write.

Families 2–5 originated in Germany. All affected family members exhibited, to varying degrees, shortening of the terminal phalanges of digits 2–5 on the hands and feet, with nail hypoplasia and distal symphalangism of the affected rays. In family 5, BDB was diagnosed, after birth, in the child with missing distal phalanges and nails and hypoplastic middle phalanges of digits 2–5. The parents and/or other family members from family 5 are not affected.

DNA Collection, Genotyping, and Mutation Detection

Informed consent was given by all participating individuals. DNA was isolated from venous blood samples, by use of standard procedures. Genotype analysis was performed for individuals from family 1, with simple sequence repeat–polymorphism markers located on

chromosome 9q22. Markers were amplified in 10-μl reactions containing 1 × PCR buffer, 200 μM of each dNTP, 0.2 μM of each primer, and 0.25 units of *Taq* polymerase. All forward primers were end-labeled with [^{32}P] by means of T4 polynucleotide kinase. PCR products were separated by denaturating-gel electrophoresis and were detected by autoradiography (X-OMAT LS; Kodak Scientific Imaging Films).

The intron-exon structure of *ROR2* and the flanking intron sequences of exons 2–9 were determined by direct sequencing of *Eco*RI subclones in pUC18, derived from the PAC RPCI-1-9h23. Primers were designed in the flanking intron sequences to amplify exons 2–8 (table 1). Exon 9, containing the TK, ST1, PR, and ST2 domains, was amplified in overlapping segments. PCR was performed in 50-μl reactions containing 1 × PCR buffer, 1.5 mM $MgCl_2$, 100 μM of each dNTP, 1 μM of each primer, and 5 units of *Taq* polymerase. The PCR conditions included an initial denaturation for 4 min at 94°C, followed by 35 cycles for 1 min at 94°C, 1 min at 58°C, 1 min at 72°C, and a final extension for 10 min at 72°C. The primer annealing temperature for exon 6 and the 3′ end of exon 9 was 63°C. The analysis of PCR products was performed on 2% agarose gels. After PCR, the DNA was purified with a PCR extraction kit (Qiagen) or was precipitated with ammonium acetate. PCR products were sequenced with the BigDye terminator kit (PE Biosystems) and were analyzed on an ABI 377 sequencer (PE Biosystems). Every mutation was confirmed by sequencing the product of an independent PCR. Restriction digests were performed in those cases in which the mutation introduced a new restriction-enzyme site or abolished a site present in the wild-type (wt) DNA (*Mwo*I digest in family 1, *Bsa*I digest in family 2, and *Acc*I digest in family 5). The PCR products from families 2–4 were subcloned (TOPO TA Cloning Kit; Invitrogen) and were sequenced. In families 1 and 2, lymphoblastoid cell lines were established, and RNA was extracted using Trizol Reagent (GibcoBRL). RNA was reverse transcribed in 40-μl reactions containing 1 × reverse transcription–PCR (RT-PCR) buffer, 100 μM DTT, 80 units RNase inhibitor, 250 μM of each dNTP, 5 μM Oligo dT primer, and Moloney murine leukemia virus 2 μl (800 units) reverse transcriptase (GIBCO), followed by PCR with oligonucleotides located in exon 8 (gat tct gta cat ctt ggt cc) and exon 9 (ctc cgc ttt gtc ctt cag c). RT-PCR was performed with an annealing temperature of 60°C, a $MgCl_2$ concentration of 3.5 mM, and 37 cycles. For family 1, allele-specific digestion of RT-PCR products was performed with *Mwo*I, as above. The intensity of individual bands was analyzed on a 2% agarose gel. To test for the mutation in family 2, a total of 98 unrelated individuals were analyzed for presence of the wt sequence of the 5′ splice site of intron 8, by digestion of PCR-amplified DNA with *Bsa*I, which cuts the wt allele into two fragments, of 271 bp and 113 bp. The *Bsa*I recognition site (ggtctc) covers the entire 5′ splice site up to and including nucleotide +5.

Results

Identification of Mutations in ROR2

Family 1 was tested for linkage to the locus reported elsewhere (Gong et al. 1999; Oldridge et al. 1999), and individual IV/1 in this family was tested for possible homozygosity. Using a set of markers spanning this region, we were able to demonstrate linkage to chromosome 9q22 in family 1. Complete linkage was shown for markers *D9S1680* and *D9S1786,* and recombination events were defined by markers *D9S1865* and *D9S1690* (data not shown). These results are consistent with previous findings. Individual IV/1 was homozygous for a contiguous series of markers spanning >15 cM from *D9S1680* to *D9S1786,* confirming the suspected homozygosity of the BDB locus.

DNA sequence analysis of *ROR2* in families 1–5 revealed heterozygous and homozygous mutations in two distinct regions of the gene. The mutations are shown in figure 3; their location in relation to the overall structure of the ROR2 protein is shown in figure 4. Ten affected members from family 1 were subjected to mutation analysis, and all of them revealed a 5-bp deletion, 1321–1325del(CGGCG), in exon 8. Direct sequencing of PCR products and restriction-enzyme digestion specific for the mutation confirmed homozygosity for this mutation in individual IV/1. The mutation is predicted to result in a frameshift and a premature termination codon after 13 amino acids. In family 2, three affected individuals were analyzed, and all of them revealed a 3-bp (CTC) deletion, which was replaced by a 19-bp fragment insertion (TACATTGTGTAAGCACAAA) at the 5′ (donor) splice site of intron 8 (IVS8+3 to +5del3ins19). For family 3, mutation analysis was performed in four affected members, and all of them exhibited an insertion, 1398–1399insA, resulting, again, in a frameshift and in a premature termination codon after 58 amino acids. Mutation analysis in family 4 revealed a mutation identical to that of family 3. The 1398–1399insA was confirmed by the subcloning and sequencing of individual clones from different PCRs. The affected individual from family 5 had a de novo nonsense mutation, 2278C→T (Q760X).

The intronic sequence of the 5′ donor site of intron 8 mutated in family 2 was tested in 98 healthy unrelated control individuals, by digestion of PCR products of exon/intron 8 with the restriction enzyme *Bsa*I. Differences from the wt sequence could not be detected, indicating that this sequence is not commonly polymorphic. To investigate the effect of the mutation on splicing,

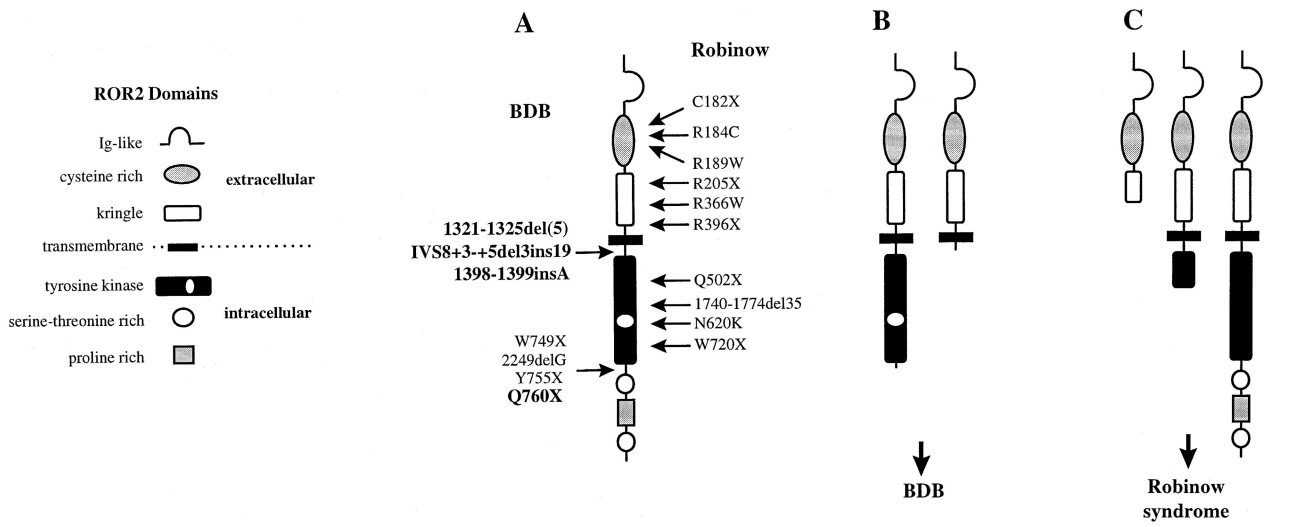

Figure 4 ROR2-protein domains and model for predicted consequences of *ROR2,* mutations. *A,* Normal structure of ROR2, showing immunoglobulin-like, cysteine-rich, kringle, transmembrane, TK (active center *white circle*), serine-threonine–rich, and proline-rich domains. The mutations causing BDB are shown on the left; mutations causing Robinow syndrome are on the right. The mutations reported in this article are in boldface; all others have been published elsewhere (Afzal et al. 2000; Oldridge et al. 2000; van Bokhoven et al. 2000). *B,* Schematic of the BDB mutations located distal (*left*), as in family 5, and proximal (*right*) to the TK domain, as described for families 1–4. Truncation of the intracellular serine-threonine–rich and proline-rich domains, as well as truncation of the entire intracellular portion of ROR2, results in dominant BDB. *C,* In contrast (left to right), extracellular truncation of ROR2, truncation within the TK domain, or selective inactivation of TK activity, which lead to autosomal recessive Robinow syndrome.

we performed RT-PCR from lymphoblastoid cells with primers spanning the exon 8/exon 9 boundary. The PCR products were subcloned, and individual clones were sequenced. We identified several mutant clones containing a 10-bp insertion between exons 8 and 9, which indicates that the inserted intronic sequence "gtaag," instead of the mutated site, had been used as a splice site. The 10-bp insertion results in a frameshift at a position very close to the mutations in families 1, 3, and 4. The frameshift leads to a predicted premature stop codon after 67 amino acids.

To analyze the stability of the mutant RNA molecule, we amplified, from total RNA obtained from lymphoblastoid cell lines of a heterozygote, the mutation-containing region in family 1. The product was digested with the restriction enzyme *Mwo*I and was run on an agarose gel to separate the wt from the mutant allele. The presence of both alleles at similar levels excluded major transcript instability (fig. 3).

Three new polymorphisms were identified: one nonsynonymous (733G→A, encoding an Ala245Thr substitution) and two synonymous (498T→C and 2154C→T). They were identified in a heterozygous or homozygous state in unaffected individuals and thus were considered to be phenotypically neutral. The GenBank accession numbers for the *ROR2* sequences (exons and flanking intron sequences) reported in this study are AF279755–AF279762.

Genotype-Phenotype Correlation

In the families presented here, BDB is inherited in a dominant fashion with full penetrance. We observed marked variability in phenotypic expression, ranging from an amputation-like phenotype, with absence of nails and distal phalanges of fingers 2-5 to a much milder phenotype comprising merely slightly shortened terminal phalanges and nails, symphalangism, and, in some cases, camptodactyly. To quantify the variability in phenotypic expression, we classified individual hands of affected family members into four groups: (1) mild (distal phalanges and nails present but hypoplastic and distal symphalangism frequent); (2) moderate (nails and/or distal phalanges absent in one or two fingers); (3) moderately severe (nails and/or distal phalanges absent in three fingers); and (4) severe (amputation-like phenotype, with absent distal phalanges and/or nails of fingers 2–5). Figure 5 gives examples of the four categories. Using this classification, we compared the families that we studied with families studied by others (Oldridge et al. 2000), to identify a possible genotype-phenotype correlation between the distal and the proximal mutations. We were able to demonstrate a clear difference in severity between the two types of mutations, with the distal mutations being less variable and more severe. The results are shown in table 2. Our results extend the published BDB phenotype toward the milder end of the spectrum and

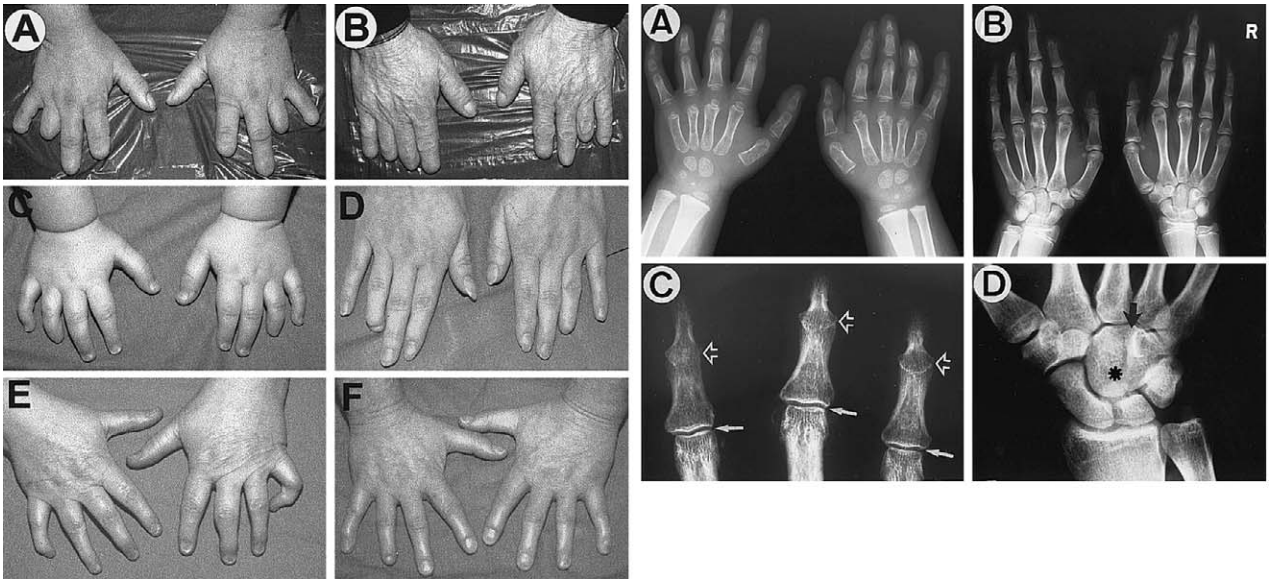

Figure 5 *Left,* Phenotypic spectrum of BDB mutations located proximal to the TK domain (family 1 *A* and *B* and family 3 *C–F*), demonstrating the different degrees of severity (designated grades 1–4, as described in the Results section). The severe phenotype (grade 4) is shown in *A*. Note complete absence of distal phalanges and nails in fingers 2–5. The moderately severe phenotype (grade 3), characterized by absence of nails and/or terminal phalanges in three fingers, is present in the left hand and is shown in *B,* whereas the right hand of this patient exhibits the severe phenotype. The intermediate type (grade 2) is shown in *C* and *D*. *C,* Absence of distal phalanges of finger 4 and hypoplasia of distal phalanges of fingers 2, 3, and 5, in a child (III/4). *D,* Individual II/3, with bilateral shortening of distal phalanges and hypoplasia/absence of nails, primarily of 4th finger. *E,* Individual I/1, with the mild phenotype (grade 1), showing moderate hypoplasia of distal phalanges, normal nails, but distal symphalangism of fingers 2–5 and camptodactyly of finger 5. *F,* Individual II/6, showing the intermediate phenotype, with absence of the distal phalanx of digit 4 of the right hand (grade 2), bilateral distal symphalangism of fingers 2–5, short fingers, but normal nails on the left hand (grade 1). *Right,* Radiographs of individuals of family 3. *A,* Bilateral hypoplasia of distal phalanges 2, 3, and 5, and absence of distal phalanx 4 of individual III/4 (also shown in *Left, C*). The metacarpal bones, proximal phalanges, and thumbs are shaped regularly. *B,* Individual III/2, with loss of distal phalanges of fingers 2 and 4 and distal symphalangism of finger 3 and finger 5 of the left hand. *C,* Magnification of radiograph showing distal part of fingers of individual II/3 (also shown in *Left, E*). Note distal symphalangism (*open arrow*) with "fusion" of distal and middle phalanges of fingers 2–4. In comparison, the joint between proximal phalanges and metacarpals has developed normally (*arrow*). *D,* Magnification of carpal bones of individual II/6 (also shown in *Left, F*). Note fusion of hamate with capitate (*asterisk*), (note line of fusion [*arrow*]) and trapezium with trapezoid of carpus.

show that distal and proximal mutations fall into distinct clinical categories.

Discussion

Vertebrate limb formation is controlled by a complex network of regulatory genes. The recent identification of the genetic basis for several human limb-malformation syndromes has yielded new insights into the pathobiology of human disease as well as into general mechanisms of limb development (Innis and Mortlock 1998; Manouvrier-Hanu et al. 1999). Among the diverse group of human limb malformations, brachydactylies are a separate entity, characterized by shortening of the digits that is due to abnormal development and/or growth of the phalanges and/or metacarpals. Brachydactylies may occur as an isolated trait or as part of a complex syndrome. BDB is the most severe of the brachydactylies and is characterized by hypoplastic/absent terminal phalanges and nails, hypoplastic middle phalanges, and symphalangism.

BDB has been associated with nonsense and frameshift mutations in *ROR2* (Oldrigde et al. 2000), a member of the Ror receptor family, which includes the paralogous gene *ROR1* (Masiakowski and Carroll 1992), and with putative orthologues in *Drosophila Dror* (Wilson et al. 1993) and *Dnrk* (Oishi et al. 1997) and *Caenorhabditis elegans CAM-1* (Forrester et al. 1999). *ROR2* encodes a putative RTK, consisting of extracellular immunoglobulin-like, cysteine-rich, and kringle domains, a transmembrane domain, an intracellular TK domain, and two carboxy-terminal serine-threonine–rich regions surrounding a proline-rich domain (schematic shown in fig. 4*A*). The mutations reported previously cluster within a distinct 7-amino-acid segment directly 3′ of the TK domain–coding region. Our results confirm the association between *ROR2* mutations and BDB, extend the previously known BDB phenotype, by

Table 1

***ROR2* Genomic Primer Sequences**

Exon	Forward	Reverse	Product Length (bp)
2	gtc tta tcc ctc tgt gtt ttc ta	cag gca atg gca gtg caa g	296
3	acg ctt gct ttt gtg acc gc	tct tgc tcg gtg gct ggg	392
4	agt gga gcc tga ggc ccg	ggt gcc cag gca acc tgg	597
5	tgg atc gca aga tgc tgg	taa aca tac agg cca gga ac	432
6	ctc tgc agc ggc ctt ca	cat ttc gag ggc cct aca c	390
7	tag ttt ggg cat gtg tag g	ccg tac aga ggc aca cc	432
8	ggt tgg tag aga act tag agt	ata att atg tgc tat gta tca ag	397
9	ctg tgg gtg ggc agg cc	acg tcc gag tgc ggc ga	503
	gag cat gat ctt cag cta ctg ttc g	cat ctc cac cac atc atg gtt g	465
	tca gac atc tgg tcc tac ggt gtg	cca tct gca ttg gga tct gc	522
	acc agc cca gtg agc aat g	gtg act gag gtc cct gtg g	574

identification of a milder heterozygous and a much-more-severe homozygous phenotype, and demonstrate that BDB can be caused not only by the previously reported distal mutations (after the TK domain) but also by mutations located proximal to the TK-coding region.

Of the four novel mutations that we have identified, the mutation in family 5 is a nonsense mutation located in the middle part of exon 9, close to the previously described mutations. However, the mutations in families 1–4 cluster in a distinct region of the protein. In families 1, 3, and 4, the mutations result in frameshifts located around the exon 8/exon 9 boundary and in subsequent premature stop codons. The mutation in family 2 alters the third and fourth position of the intron 8 splice-donor site by replacing 3 bp by a 19-bp fragment of unknown origin (i.e., IVS8+3 → +5del3ins19). The inserted sequence contains a perfect consensus splice-donor site (gtaag) 10 bp downstream of the wt site. Our experiments using RT-PCR from lymphoblastoid cells have demonstrated that this new site is used, resulting in the insertion of three amino acids, a frameshift, and a premature stop codon. Thus, the location of the frameshift in family 2 is very similar to the locations of those in families 1, 3, and 4. Studies in yeast and of human genetic disorders have demonstrated that messages containing premature translation–termination codons are, depending on their location, frequently subject to degradation (Hentze and Kulozik 1999). If the position of the premature termination codon is ⩾50 bp 5′ of the final exon/intron junction, the message will be degraded, whereas stop codons 3′ of this boundary are usually stable (Thermann et al. 1998; Zhang et al. 1998). The mutations reported here result in termination codons located 3′ of this boundary and are thus likely to be stable. This is supported by our demonstration in family 1 (which harbors the most 5′ of the mutations described here) of approximately equal amounts of normal and mutant message in RNA from lymphoblastoid cells. Translation of the mutant messages will thus either lead to a truncated receptor that lacks the entire intracellular portion including the TK domain (families 1–4) or, as in family 5, result in loss of the carboxy-terminal serine-proline–rich and threonine-rich domains, leaving the TK intact (fig. 4*B*).

Table 2

Comparison of Grades of Severity in Hands of Patients with a Proximal and a Distal Mutation

	Grade of Severity				
Mutation (Family)[a]	1	2	3	4	Total
Proximal:					
1321–1325del5 (1)	4	16	11	9	40
IVS8+3 → +5del3ins19 (2)	1	3	2		6
1398–1399insA (3)	4	8			12
1398-1399insA (4)		7	2	1	10
Total	9	34	15	10	68
Distal:					4
W749X*			4	14	18
2249delG*				4	4
Y755X*			7	35	42
Q760X (5)				2	2
Total	0	0	11	55	66

[a] The mutations indicated with an asterisk (*) are from the study by Oldridge et al. (2000).

We compared the phenotype of patients with the distal and proximal mutation and were able to demonstrate a significant difference between the two groups. The distal mutations invariably result in the classic severe, amputation-like phenotype, affecting three or more fingers. In contrast, patients with the proximal mutation are generally less severely affected and have a more variable phenotype (table 2). The phenotypic overlap between the two groups indicates that the two types of mutation have similar consequences for protein function.

Both the dominant effect of the BDB mutations and their clustering within two distinct regions of the gene, resulting in truncated receptors, suggest a molecular pathology that is distinct from simple haploinsufficiency. This is supported by several lines of evidence. In the mouse, heterozygous inactivation of *Ror2* ($Ror2^{+/-}$) produces no phenotype. Homozygous inactivation of $Ror2^{-/-}$ leads to a severe, neonatal lethal skeletal dysplasia, with profound shortening and deformation of all bones that undergo endochondral ossification (DeChiara et al. 2000; Takeuchi et al. 2000). The middle phalanges are missing, but the distal phalanges appear normal. In contrast, patients heterozygous for the BDB mutation have a distinct acral phenotype with missing distal phalanges, although the remainder of the skeleton is normal. In the homozygous patient, this phenotype is even more pronounced, and it results in a complete loss of distal digital structures. The phenotype of this patient, along with those of the other patients with BDB, supports the concept that BDB is caused by a mechanism that is distinct from that in the $Ror2^{-/-}$ mouse.

Although the limb phenotype in the homozygous patient can be interpreted as a severe form of BDB, the patient has several other changes that are not part of the known BDB spectrum. The severe mesomelic shortening of the limbs, the alterations of the thoracic spine, and the heart defect are additional findings that share some similarity with Robinow syndrome (MIM 268310). Features of this complex syndrome include a characteristic facies with large, prominent eyes, hypertelorism, macrocephaly, short nose with anteverted nostrils, long philtrum, and a triangular mouth (giving the appearance of a "fetal face"), short stature, mesomelic shortening of the arms, variable malformations of the hands, vertebral and rib anomalies, hypoplastic external genitalia, heart defects, and, in some cases, developmental delay. Very recent findings (Afzal et al. 2000; van Bokhoven et al. 2000) suggest that the recessive form of Robinow syndrome is caused by mutations in *ROR2* and is therefore allelic to dominantly inherited BDB. The homozygous individual reported here lacks most of the typical craniofacial features of Robinow syndrome, exhibits a different limb phenotype, and, therefore, does not have Robinow syndrome, as one would expect in light of the homozygosity of his mutation. However, certain features of his phenotype overlap with those found in Robinow syndrome. Vertebral and rib anomalies, brachymelia of the arms, hypertelorism, hyperplastic alveolar ridges, and a heart defect are present in our patient and are part of the Robinow spectrum. Hence, this individual represents a phenotypic and genotypic link between autosomal recessive Robinow syndrome and BDB.

In contrast with BDB, Robinow syndrome is caused by homozygous mutations that are scattered throughout the entire coding region (fig. 4*C*) (Afzal et al. 2000; van Bokhoven et al. 2000). The Robinow mutations reported so far fall into three categories: missense mutations that are located in the extracellular domains and that probably interfere with ligand-receptor or other protein-protein binding, nonsense mutations that are located in the extracellular domains and that are predicted to result in a total loss of ROR2 function, and missense mutations or frameshifts within the TK domain that inactivate the TK activity. Interestingly, the proximal BDB mutations reported here (families 1–4) delete the entire intracellular portion of ROR2 and will thus also result in a loss of TK function. However, in contrast with the Robinow mutations, in which at least part of the nonfunctional TK domain is retained, these proximal BDB mutations result in loss of the entire TK domain. Thus, deletion of the carboxy-terminal serine-threonine–rich and proline-rich domains, as in family 5 and in the report by Oldridge et al. (2000), or deletion of the entire intracellular portion of ROR2, including the TK domain, has similar consequences and results in dominant BDB. In contrast, inactivation of the TK or partial deletion of the TK domain, including the carboxy-terminal domains, has an effect comparable to the inactivation of the entire ROR2 receptor and results in recessive Robinow syndrome (see fig. 4*B* and *C*).

It can be concluded that mutations in *ROR2* account for distinct defects depending on the nature and the location of the mutation. Heterozygous loss-of-function mutations appear to be without consequences, as demonstrated by the lack of BDB in individuals with chromosomal deletions involving *ROR2,* by the lack of a phenotype in carriers of Robinow syndrome mutations, and by the absence of a phenotype in $Ror2^{+/-}$ mice. In contrast, the BDB mutations are dominant. On binding of their ligand, all known RTKs (with the exception of the insulin receptor) undergo a transition from a monomeric to a heteromeric state, resulting in autophosphorylation and subsequent activation of intracellular messenger molecules (Lemmon and Schlessinger 1994). By analogy to other RTKs, the BDB mutations may have a dominant effect (negative or positive), by altering signaling of their wt dimerization partners. The distinct phenotype of our homozygous patient and the lack of a BDB phenotype in Robinow syndrome suggest that the mutant ROR2 molecule interacts with other, yet unknown partners. In vitro and in vivo experiments expressing the mutations described here will help us to study this hypothesis.

Acknowledgments

We thank all family members for participating in the project. The skillful support from Britta Hoffmann is appreciated. We thank Leonore Senf and Kristina Reitz for assistance. M.O.

and A.O.M.W. were supported by the Wellcome Trust. The RPCI1 PAC library was provided by the HGMP Resource Centre. This work was funded by a grant from the Deutsche Forschungsgemeinschaft to S.M.

Electronic-Database Information

The accession number and URLs for data in this article are as follows:

GenBank, http://www.ncbi.nlm.nih.gov/Genbank/index.html
Online Mendelian Inheritance in Man (OMIM), http://www.ncbi.nlm.nih.gov/Omim (for BDB [MIM 113000])

References

Afzal AR, Rajab A, Fenske CD, Oldridge M, Elanko N, Ternes-Pereira E, Tüysüz B, Murday VA, Patton MA, Wilkie AO, Jeffery S (2000) Recessive Robinow syndrome, allelic to dominant brachydactyly type B is caused by mutation of *ROR2*. Nat Genet 25:419–422

Bell J (1951) On brachydactyly and symphalangism. In: The treasury of human inheritance. Vol 5. Cambridge University Press, Cambridge, pp 1–31

DeChiara TM, Kimble RB, Poueymirou WT, Rojas J, Masiakowski P, Valenzuela DM, Yancopoulos GD (2000) *ROR2,* encoding a receptor-like tyrosine kinase, is required for cartilage and growth plate development. Nat Genet 24:271–274

Forrester WC, Dell M, Perens E, Garriga G (1999) A *C. elegans* Ror receptor tyrosine kinase regulates cell motility and asymmetric cell division. Nature 400:881–815

Gong Y, Chitayat D, Kerr B, Chen T, Babul-Hirji R, Pal A, Reiss M, Warman ML (1999) Brachydactyly type B: clinical description, genetic mapping to chromosome 9q, and evidence for a shared ancestral mutation. Am J Hum Genet 64: 570–577

Hentze MW, Kulozik AE (1999) A perfect message: RNA surveillance and nonsense-mediated decay. Cell 96:307–310

Innis JW, Mortlock DP (1998) Limb development: molecular dysmorphology is at hand! Clin Genet 53:337–348

Lemmon MA, Schlessinger J (1994) Regulation of signal transduction and signal diversity by receptor oligomerization. Trends Biochem Sci 19:459–463

Manouvrier-Hanu S, Holder-Espinasse M, Lyonnet S (1999) Genetics of limb anomalies in humans. Trends Genet 15: 409–417

Masiakowski P, Carroll RD (1992) A novel family of cell surface receptors with tyrosine kinase-like domain. J Biol Chem 267:26181–26190

Oishi I, Sugiyama S, Liu ZJ, Yamamura H, Nishida Y, Minami Y (1997) A novel Drosophila receptor tyrosine kinase expressed specifically in the nervous system: unique structural features and implication in developmental signaling. J Biol Chem 272:11916–11923

Oldridge M, Fortuna AM, Maringa M, Propping P, Mansour S, Pollitt C, DeChiara TM, Kimble RB, Valenzuela DM, Yancopoulos GD, Wilkie AO (2000) Dominant mutations in *ROR2,* encoding an orphan receptor tyrosine kinase, cause brachydactyly type B. Nat Genet 24:275–278

Oldridge M, Temple IK, Santos HG, Gibbons RJ, Mustafa Z, Chapman KE, Loughlin J, Wilkie AO (1999) Brachydactyly type B: linkage to chromosome 9q22 and evidence for genetic heterogeneity. Am J Hum Genet 64:578–585

Takeuchi S, Takeda K, Oishi I, Nomi M, Ikeya M, Itoh K, Tamura S, Ueda T, Hatta T, Otani H, Terashima T, Takada S, Yamamura H, Akira S, Minami Y (2000) Mouse *Ror2* receptor tyrosine kinase is required for the heart development and limb formation. Genes Cells 5:71–78

Thermann R, Neu-Yilik G, Deters A, Frede U, Wehr K, Hagemeier C, Hentze MW, Kulozik AE (1998) Binary specification of nonsense codons by splicing and cytoplasmic translation. EMBO J 17:3484–3494

van Bokhoven H, Celli J, Kayserili H, van Beusekom E, Balci S, Brussel W, Skovby F, Kerr B, Percin EF, Akarsu N, Brunner HG (2000) Mutation of the gene encoding the ROR2 tyrosine kinase causes autosomal recessive Robinow syndrome. Nat Genet 25:423–426

Wilson C, Goberdhan DC, Steller H (1993) *Dror,* a potential neurotrophic receptor gene, encodes a Drosophila homolog of the vertebrate *Ror* family of Trk-related receptor tyrosine kinases. Proc Natl Acad Sci USA 90:7109–7113

Zhang J, Sun X, Qian Y, LaDuca JP, Maquat LE (1998) At least one intron is required for the nonsense-mediated decay of triosephosphate isomerase mRNA: a possible link between nuclear splicing and cytoplasmic translation. Mol Cell Biol 18:5272–5283